U.S. DEPARTMENT OF ENERGY | Office of Science

NSTX-U

Modelling of VDEs with M3D-C1

D.Pfefferlé[1]

S.Jardin[1] **N.Ferraro[1]** **C.Myers[1]** **A.Bhattacharjee[1]**

[1] *PPPL, Princeton 08540 NJ, USA*

APS-DPP 2016
San Jose, CA
November 1, 2016

PPPL

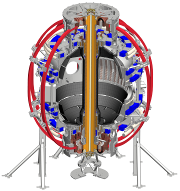

VDEs are inherent to diverted tokamak plasmas

external potential from PF coils

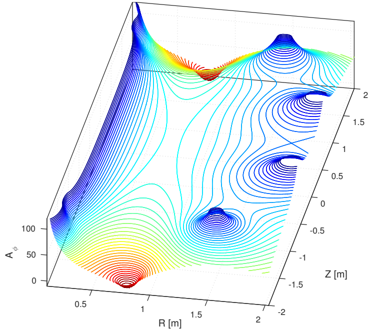

effective potential along Z

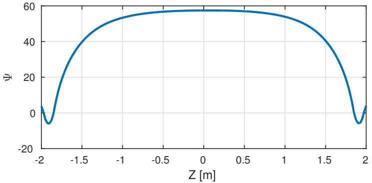

- diverted plasma on a saddle due to external field (PF coils) ⇒ elongation, vertically unstable equilibrium
- conducting structures do not allow fast flux changes ⇒ passive stabilisation + feedback control
- loss of vertical control leads to deleterious contact with wall
  - transfer/induction of current from core → halo → wall ⇒ forces and stresses
  - scraping-off of $q_{edge} < 2$ ⇒ 3D instabilities (kink), toroidal peaking of forces
  - thermal collapse, impurities ⇒ breaking of flux surfaces, runaway electrons

Damaging power of VDEs calls for realistic modelling

- forces during VDEs lead to structural damages of PFCs, can result in machine shutdown
  - worst case VDE is a design drive for ITER
  - need for avoidance (preemptive measures) and mitigation (damage control)
- abundant experimental data to be analysed and interpreted
  - provide theoretical/modelling support
  - help interpret measurements and optimise diagnostics for wall/halo currents

Basic/fundamental questions:

1. What are the keys dynamics/regimes/phases of VDEs ?
   - rich literature, reduced models, linear theories, Halo/Hiro debate
   - self-consistently assembling the pieces of the puzzle is not trivial (stiffness)
2. Can we simulate/model VDEs accurately enough to feel confident about predictions for ITER ?
   - **difficult**: 2D + prescriptions OK, 3D not (yet) with realistic parameters
   - 3D: computationally far more expensive, profoundly richer physics than 2D

Phenomenology of VDEs serves as modelling targets

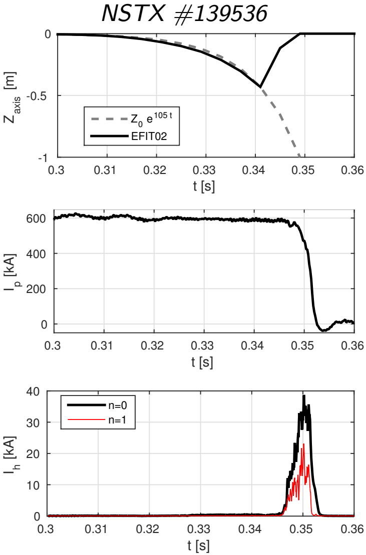

- drift phase [Pfefferlé, 2016]
  $t_D \sim (L_w/R_w)(I_p/I_d)(Z_d/Z_w)^2 \sim 30\text{ms}$
  - **slow** relaxation process
  - plasma mostly in force balance
  - advection ($\approx$ rigid body), inductive coupling with wall $\Rightarrow$ **implicit scheme**
- current quench $t_{CQ} \gtrsim L_p^*/R_p^* \sim 3ms$ [Wesley, 2006]
  - current transfer/induction from plasma to wall
  - flux scrape-off (advection-diffusion) + time-evolving resistivity via temperature
- normal wall currents $\Delta t_H \sim t_{CQ}$ [Myers, 2016]
  - shared/induced currents in resistive halo
  - early $n = 1 \sim n = 0$ components
  - counter-I_p rotation $\Omega R \sim 3\text{km/s} = 0.1 c_s$ for max 4 turns

VDEs progress through multiple phases/regimes associated with specific numerical difficulties

1. vertical drift phase (adiabatically evolving MHD equilibrium)
   - slow advection and force balance
     - fixed mesh (resolution), leading edge surface currents, spurious numerical modes
     - role of sources and sink to avoid/trigger internal instabilities (early thermal quench)
     - time-varying PF coil currents, loop voltage, pellet injection
   - plasma/wall inductive coupling and resistive decay of wall currents
     - wall shape and 3D geometry, holes and cuts (poloidal or toroidal gaps), materials with different resistivities
     - coupling with engineering code `VALEN`
2. axisymetric plasma contacting wall
3. 3D plasma contacting wall

VDEs progress through multiple phases/regimes associated with specific numerical difficulties

1. vertical drift phase (adiabatically evolving MHD equilibrium)
2. axisymetric plasma contacting wall
   - multi-region problem
   - "heat" equation for flux scrape-off
     - induced (time-varying) vs shared currents (spatially non-uniform, potential build-up)
   - fast evolution of temperature $\rightarrow$ resistivity (cold wall, hot core)
     - thermal conductivity profile
     - sharp gradients vs resolution $\Rightarrow$ **anisotropic mesh**
3. 3D plasma contacting wall

VDEs progress through multiple phases/regimes associated with specific numerical difficulties

1. vertical drift phase (adiabatically evolving MHD equilibrium)
2. axisymetric plasma contacting wall
3. 3D plasma contacting wall
   - external kink instabilities 2/1, 3/2, 1/1 (+coupling)
   - stabilising role of halo and/or Hiro currents
     - width, breadth
     - temperature → resistivity
   - deformation of flux-surfaces (equilibrium) vs formation of flux tubes (growing current-carrying islands)
   - torque and rotation
     - plasma flow, rotating instability, spinning coin
     - boundary conditions

M3D-C1 is a state-of-art FEM implicit code, suitable for modelling VDEs

Typical setup, parameters and recipe:

0.a 3 region **anisotropic mesh** for plasma, wall and vacuum

0.b Grad-Shafranov equilibrium reconstruction from experimental profiles (`geqdsk`) and coil currents

1. 2D nonlinear **implicit** runs, tuned to match realistic timescales
   - Spitzer resistivity $\times$ 30 $\Rightarrow$ Lundquist $S \sim 10^8 - 10^9$
   - 2cm wall with resistivity $\eta_w = 1.9 \times 10^{-6} \Omega m$
   - thermal conductivity $\kappa_T = 10^{-6} \kappa_0$
   - halo region: $n_h = 10^{18} m^{-3}$, $p_h = 8$ Pa, $T_h = 25$eV
     - effective temperature for halo resistivity $T_h = 9$eV
2. linear analysis launched at different times during 2D drift phase
   - monitor $n > 0$ modes, compare instantaneous growth rates with $n = 0$
3. 3D nonlinear **implicit** runs started when plasma almost contacts wall
   - 48 toroidal planes
   - 4608 cores for 300'000 CPU hours
   - still **in progress** due to NERSC queues

M3D-C1 2D nonlinear simulation of NSTX #132859

with $\eta_W = 1.9 \times 10^{-6}\Omega m$, $T_h = 9$eV

toroidal current density

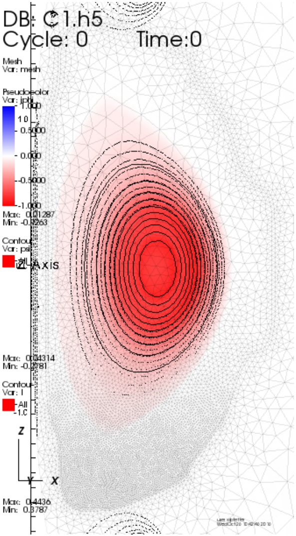

$\vec{B}_{poloidal}$ *and* j_{normal}

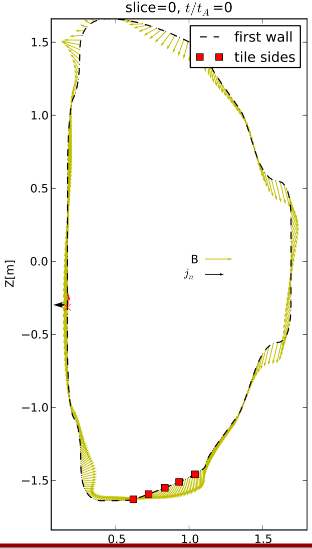

q-profile

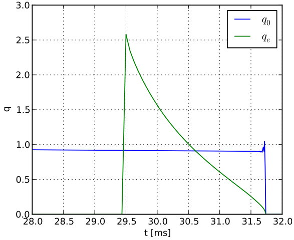

shunt tile currents

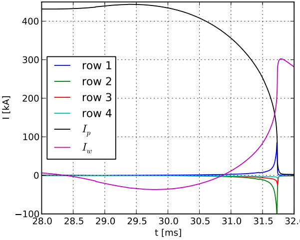

M3D-C1 2D nonlinear simulation of NSTX #132859

with $\eta_W = 1.9 \times 10^{-6} \Omega m$, $T_h = 9$eV

toroidal current density

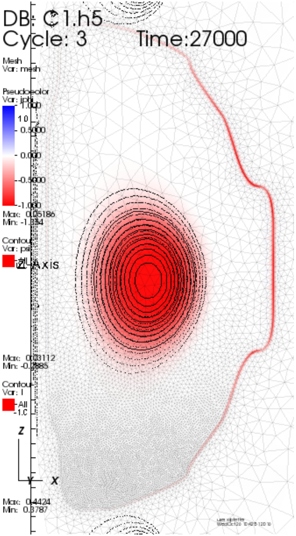

$\vec{B}_{poloidal}$ and j_{normal}

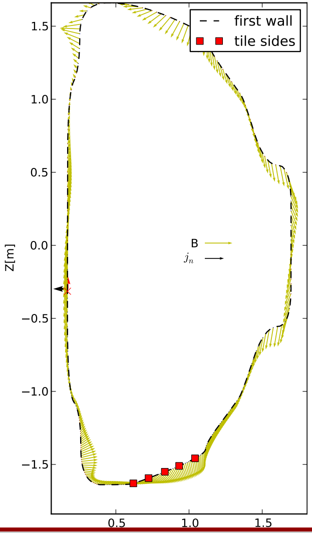

q-profile

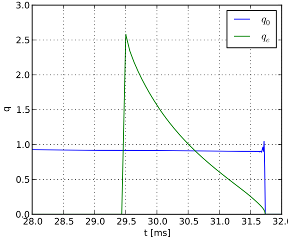

shunt tile currents

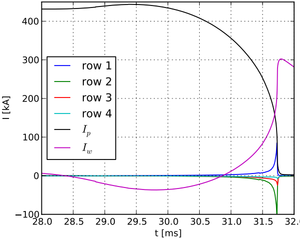

M3D-C1 2D nonlinear simulation of NSTX #132859

with $\eta_W = 1.9 \times 10^{-6} \Omega m$, $T_h = 9$eV

toroidal current density

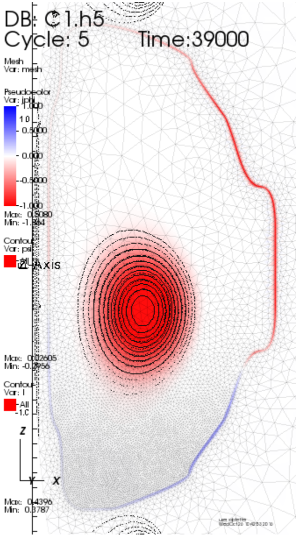

$\vec{B}_{poloidal}$ *and* j_{normal}

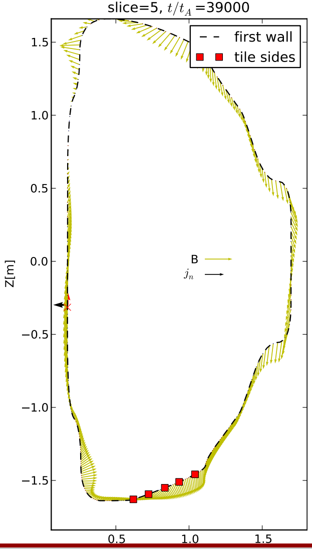

q-profile

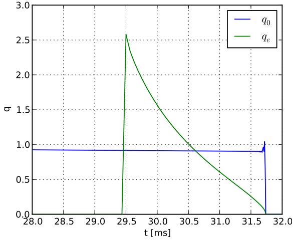

shunt tile currents

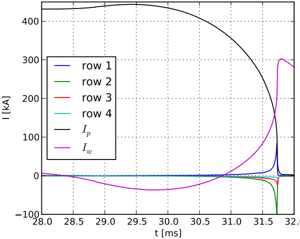

M3D-C1 2D nonlinear simulation of NSTX #132859

with $\eta_W = 1.9 \times 10^{-6}\Omega m$, $T_h = 9$eV

toroidal current density

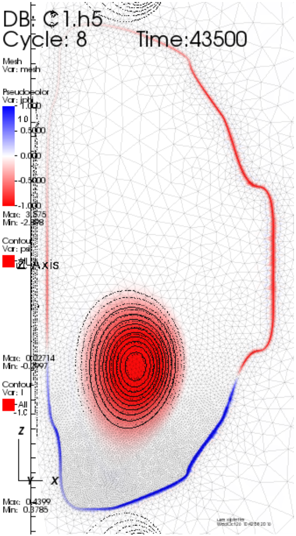

$\vec{B}_{poloidal}$ and j_{normal}

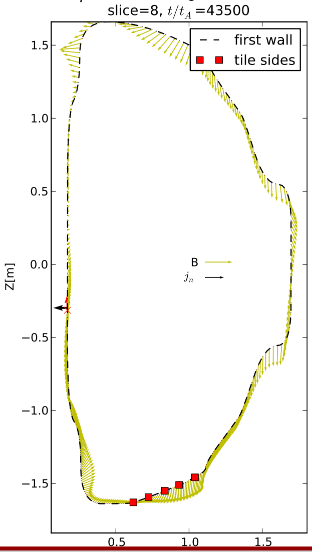

q-profile

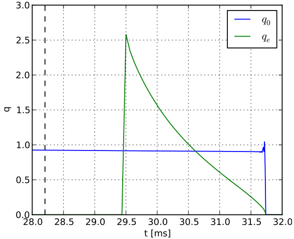

shunt tile currents

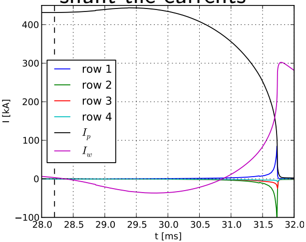

M3D-C1 2D nonlinear simulation of NSTX #132859

with $\eta_W = 1.9 \times 10^{-6}\Omega m$, $T_h = 9$eV

toroidal current density

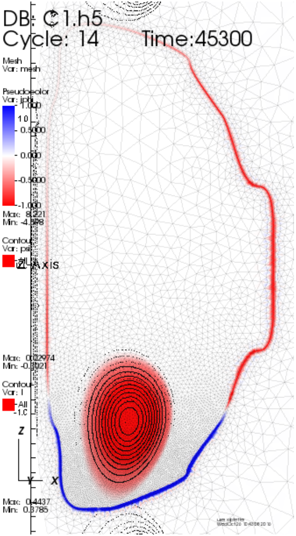

$\vec{B}_{poloidal}$ *and* j_{normal}

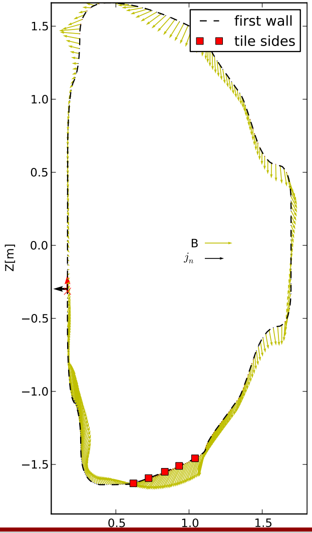

q-profile

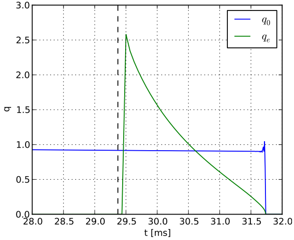

shunt tile currents

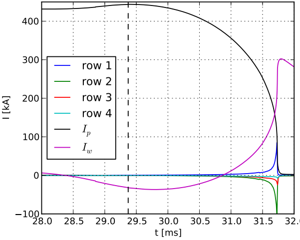

M3D-C1 2D nonlinear simulation of NSTX #132859

with $\eta_W = 1.9 \times 10^{-6}\Omega m$, $T_h = 9$eV

toroidal current density

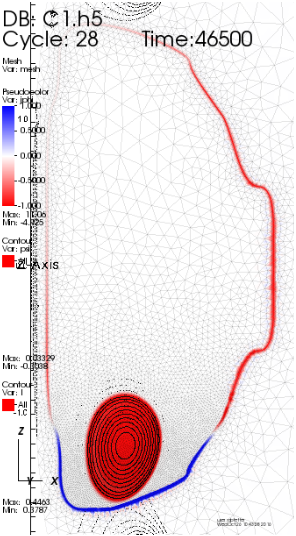

$\vec{B}_{poloidal}$ *and* j_{normal}

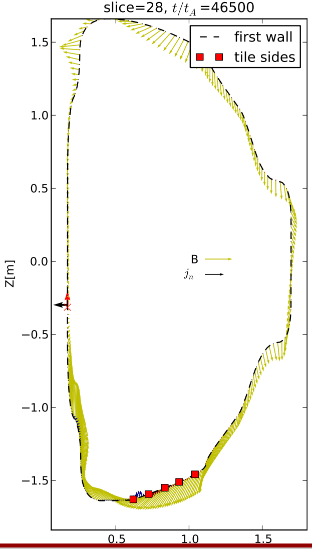

q-profile

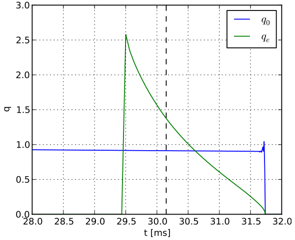

shunt tile currents

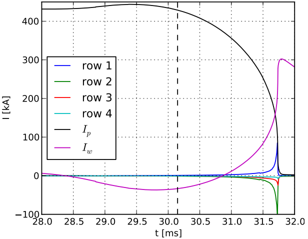

M3D-C1 2D nonlinear simulation of NSTX #132859

with $\eta_W = 1.9 \times 10^{-6}\Omega m$, $T_h = 9$eV

toroidal current density

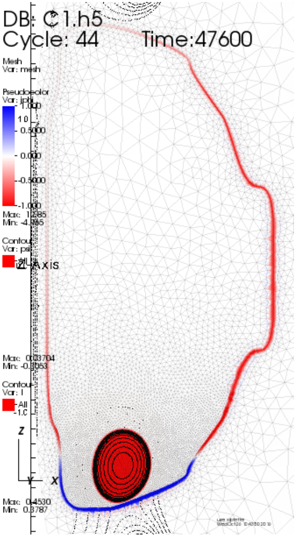

$\vec{B}_{poloidal}$ and j_{normal}

slice=44, t/t_A =47600

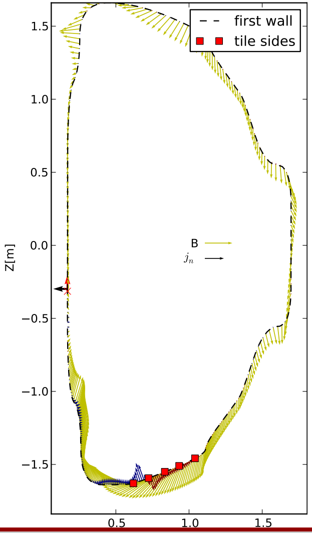

q-profile

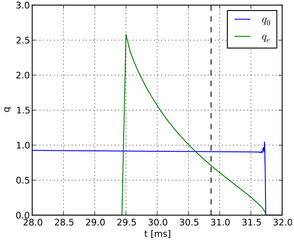

shunt tile currents

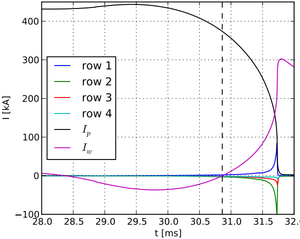

M3D-C1 2D nonlinear simulation of NSTX #132859

with $\eta_W = 1.9 \times 10^{-6}\Omega m$, $T_h = 9$eV

toroidal current density

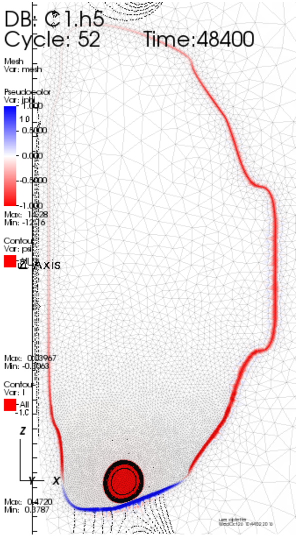

$\vec{B}_{poloidal}$ *and* j_{normal}

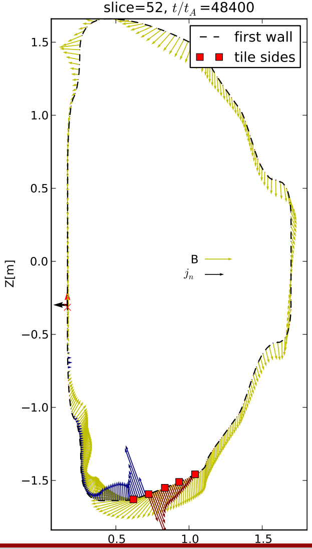

q-profile

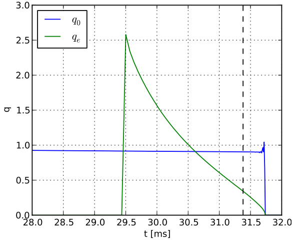

shunt tile currents

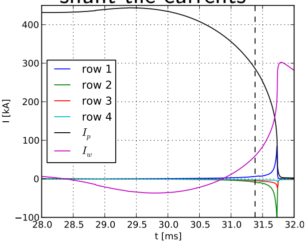

M3D-C1 2D nonlinear simulation of NSTX #132859

with $\eta_W = 1.9 \times 10^{-6}\Omega m$, $T_h = 9$eV

toroidal current density

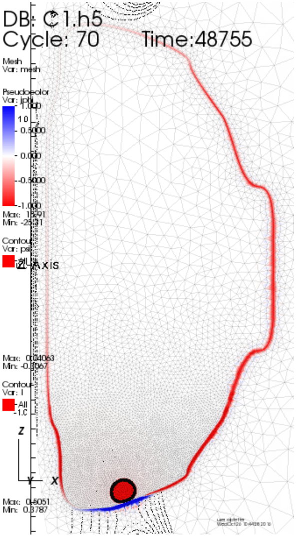

$\vec{B}_{poloidal}$ and j_{normal}

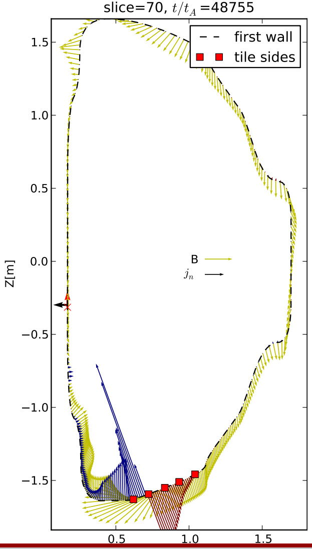

q-profile

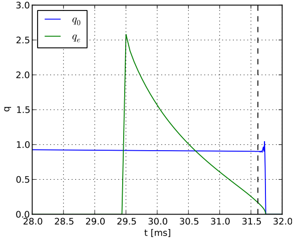

shunt tile currents

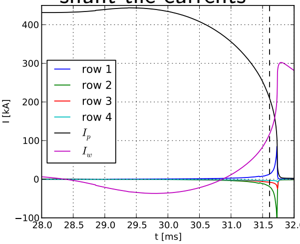

M3D-C1 2D nonlinear simulation of NSTX #132859

with $\eta_W = 1.9 \times 10^{-6}\Omega m$, $T_h = 9$eV

toroidal current density

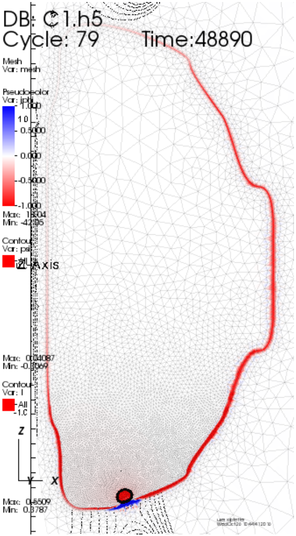

$\vec{B}_{poloidal}$ and j_{normal}

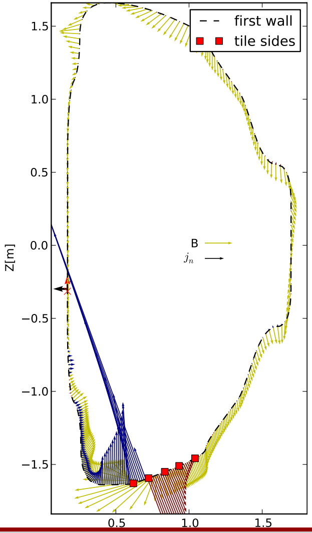

q-profile

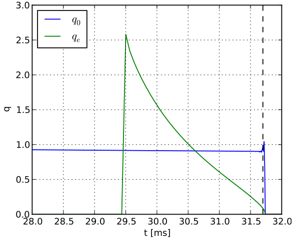

shunt tile currents

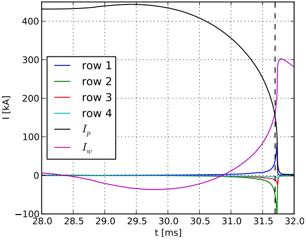

M3D-C1 2D nonlinear simulation of NSTX #132859

with $\eta_W = 1.9 \times 10^{-6}\Omega m$, $T_h = 9$eV

toroidal current density

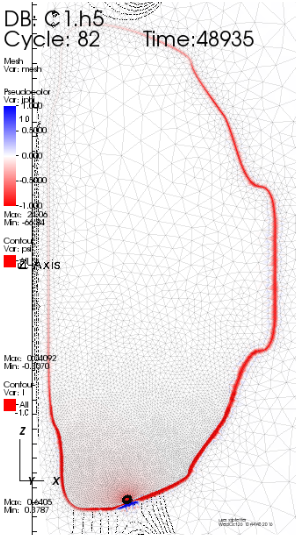

$\vec{B}_{poloidal}$ *and* j_{normal}

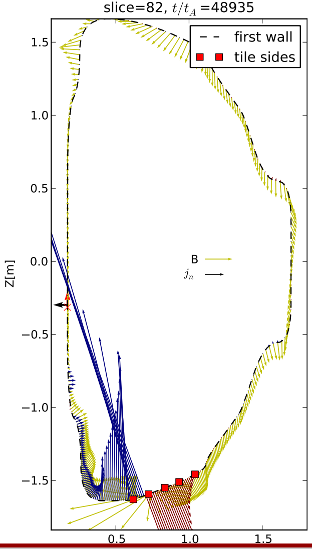

q-profile

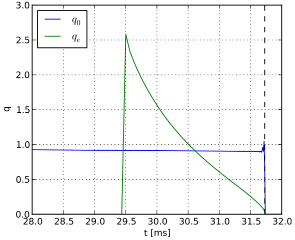

shunt tile currents

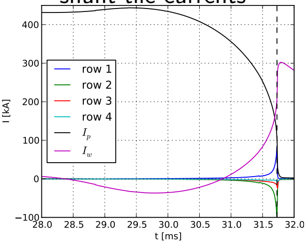

M3D-C1 2D nonlinear simulation of NSTX #132859

with $\eta_W = 1.9 \times 10^{-6}\Omega m$, $T_h = 9$eV

toroidal current density

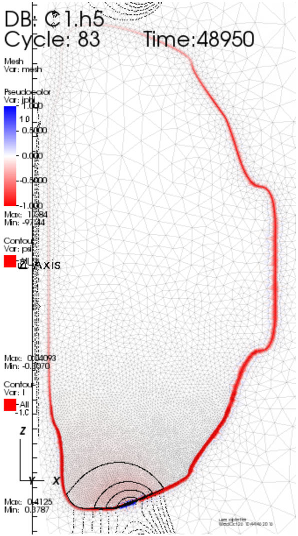

$\vec{B}_{poloidal}$ *and* j_{normal}

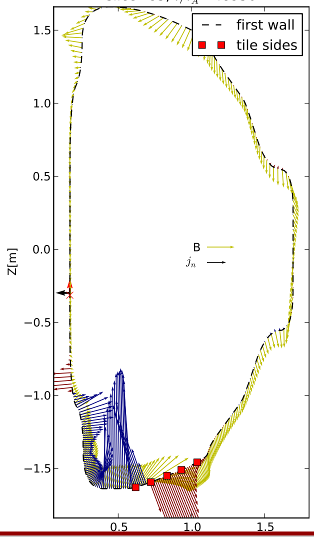

q-profile

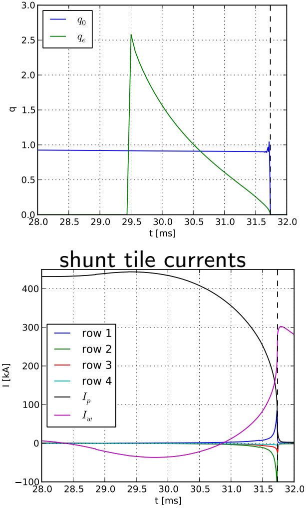

Another M3D-C1 2D nonlinear run of NSTX #132859

with $\eta_W = 5 \times 10^{-4}\Omega m$, $T_h = 24$eV

toroidal current density

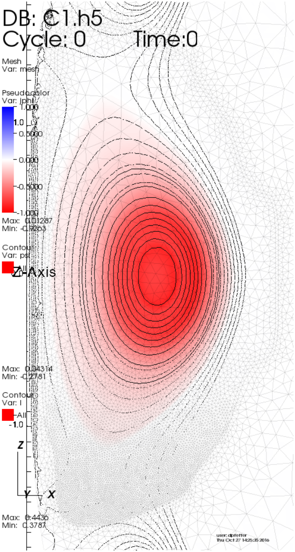

$\vec{B}_{poloidal}$ and j_{normal}

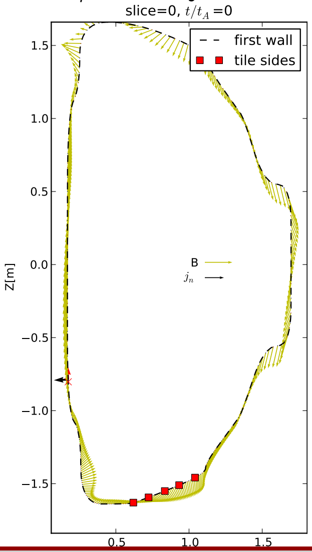

q-profile

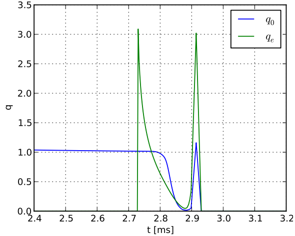

shunt tile currents

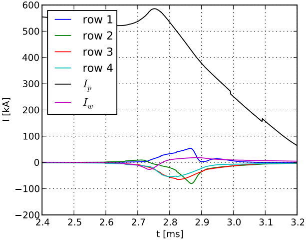

Another M3D-C1 2D nonlinear run of NSTX #132859

with $\eta_W = 5 \times 10^{-4}\Omega m$, $T_h = 24$**eV**

toroidal current density

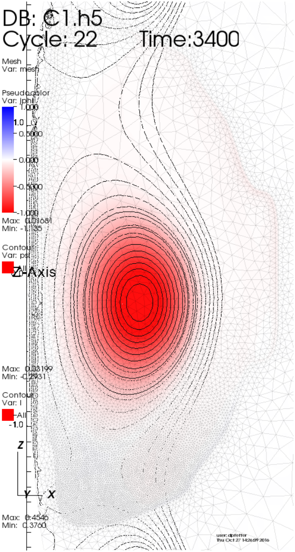

$\vec{B}_{poloidal}$ *and* j_{normal}

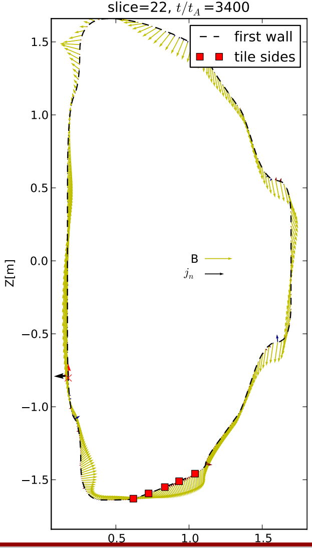

q-profile

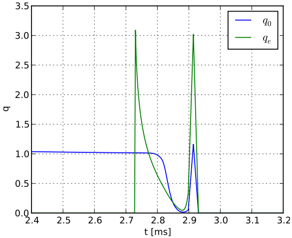

shunt tile currents

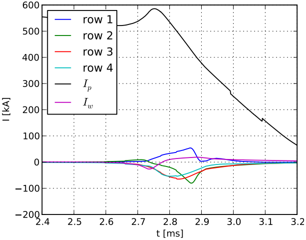

Another M3D-C1 2D nonlinear run of NSTX #132859

with $\eta_W = 5 \times 10^{-4}\Omega m$, $T_h = 24$eV

toroidal current density

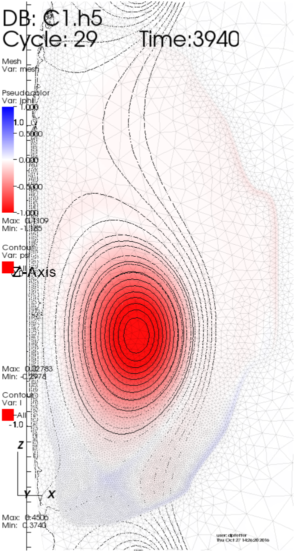

$\vec{B}_{poloidal}$ *and* j_{normal}

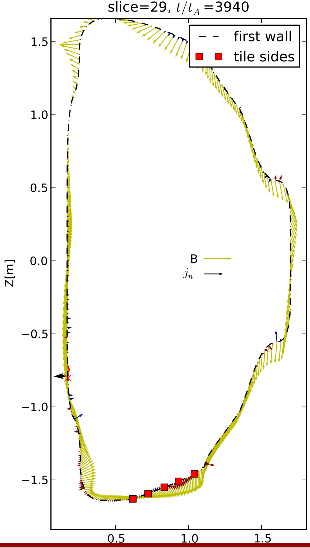

q-profile

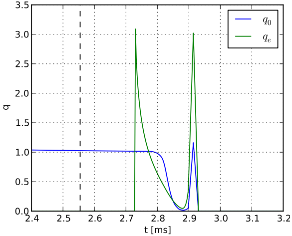

shunt tile currents

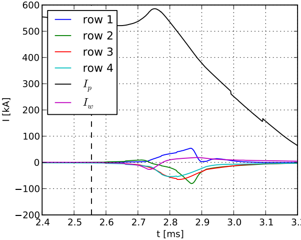

Another M3D-C1 2D nonlinear run of NSTX #132859

with $\eta_W = 5 \times 10^{-4}\Omega m$, $T_h = 24$eV

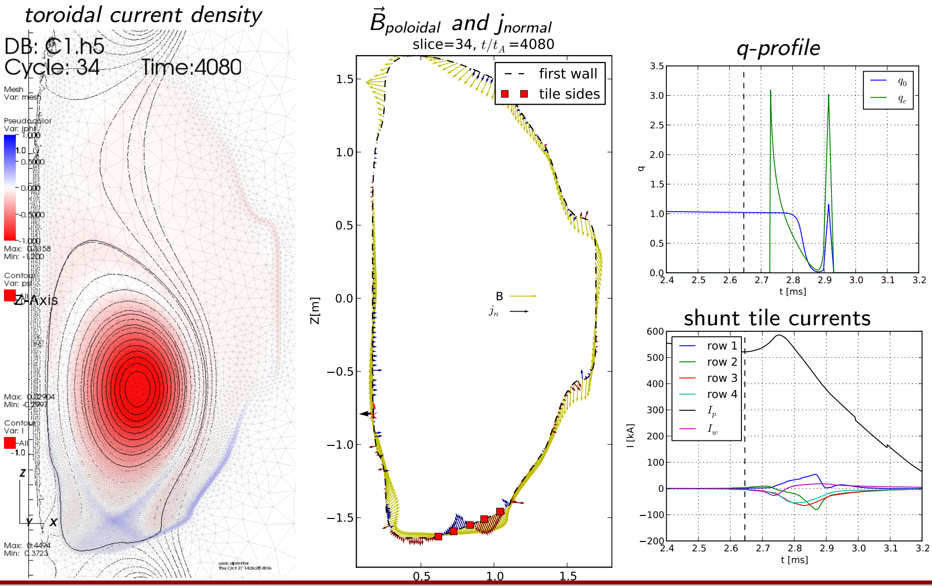

Another M3D-C1 2D nonlinear run of NSTX #132859

with $\eta_W = 5 \times 10^{-4}\Omega m$, $T_h = 24$eV

toroidal current density

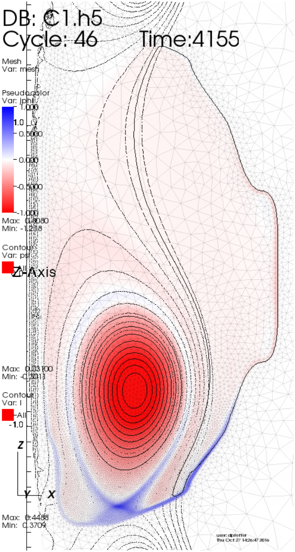

$\vec{B}_{poloidal}$ *and* j_{normal}

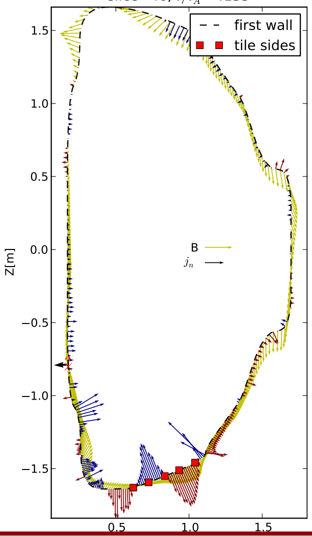

q-profile

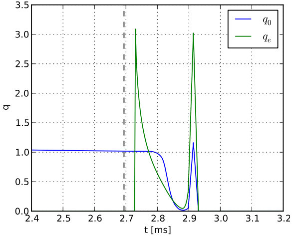

shunt tile currents

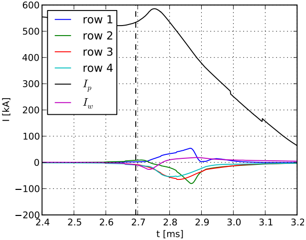

Another M3D-C1 2D nonlinear run of NSTX #132859

with $\eta_W = 5 \times 10^{-4}\Omega m$, $T_h = 24$eV

toroidal current density

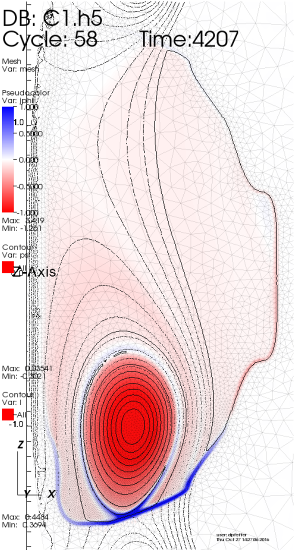

$\vec{B}_{poloidal}$ and j_{normal}

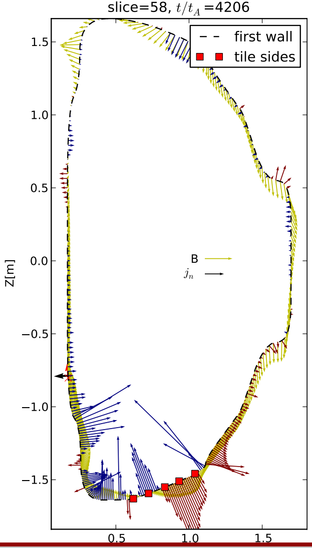

q-profile

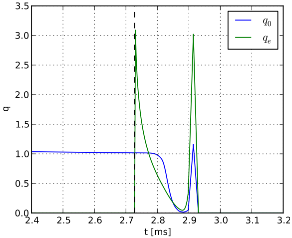

shunt tile currents

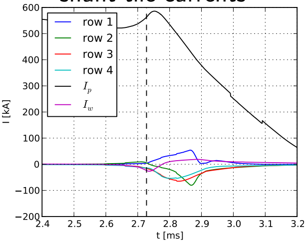

Another M3D-C1 2D nonlinear run of NSTX #132859

with $\eta_W = 5 \times 10^{-4}\Omega m$, $T_h = 24$eV

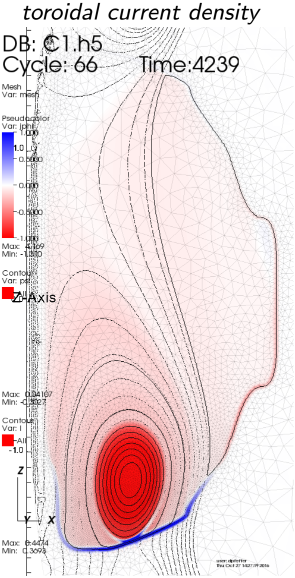

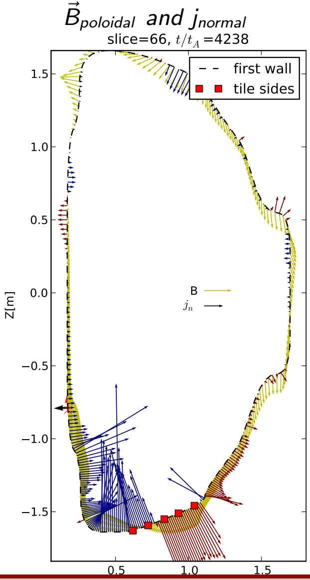

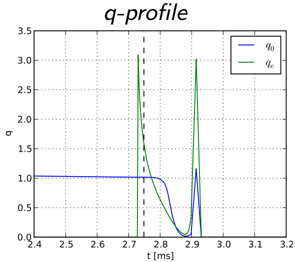

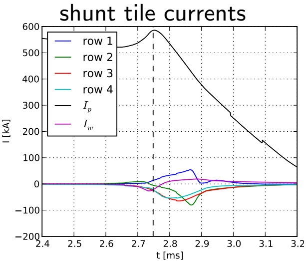

Another M3D-C1 2D nonlinear run of NSTX #132859

with $\eta_W = 5 \times 10^{-4}\Omega m$, $T_h = 24$eV

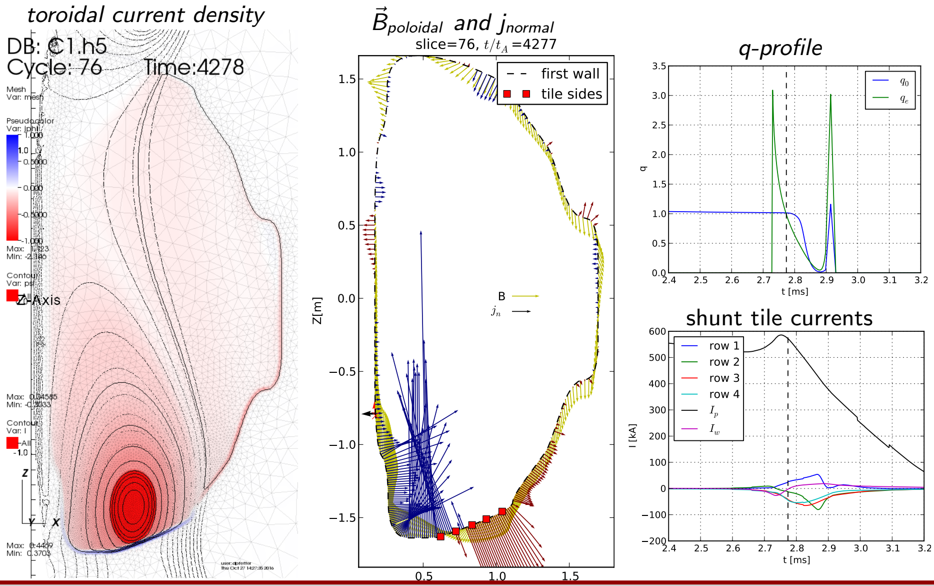

Another M3D-C1 2D nonlinear run of NSTX #132859

with $\eta_W = 5 \times 10^{-4}\Omega m$, $T_h = 24$eV

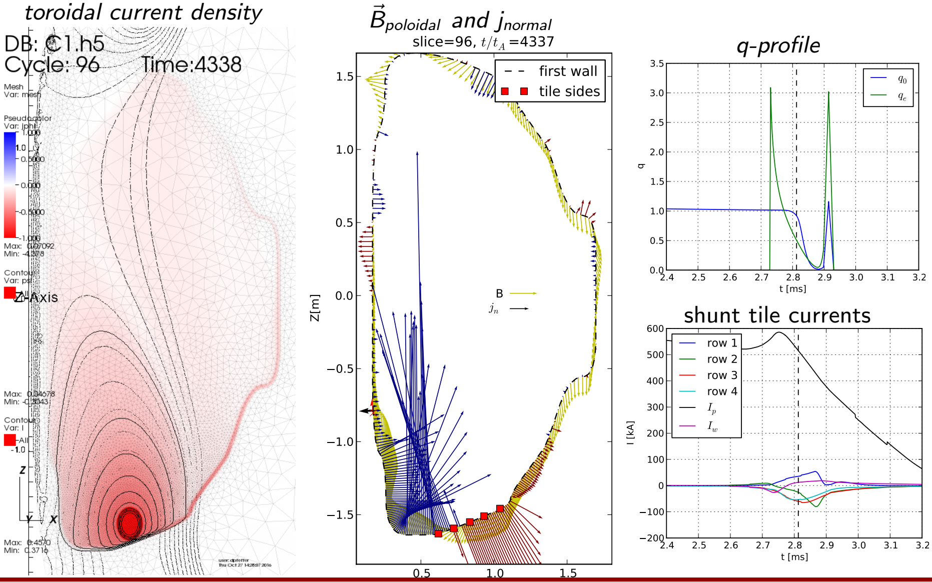

Another M3D-C1 2D nonlinear run of NSTX #132859

with $\eta_W = 5 \times 10^{-4}\Omega m$, $T_h = 24$eV

toroidal current density

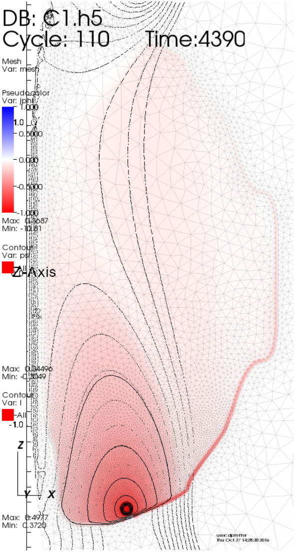

$\vec{B}_{poloidal}$ and j_{normal}

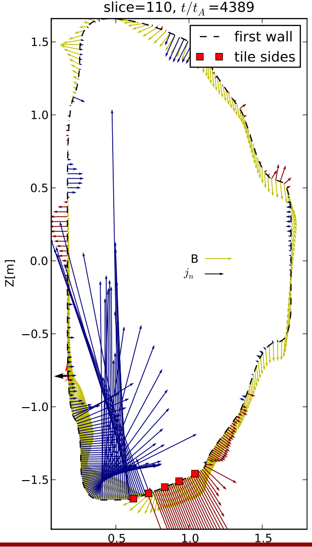

q-profile

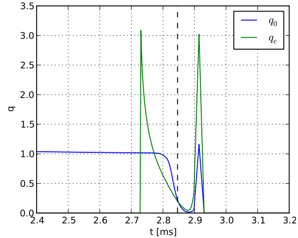

shunt tile currents

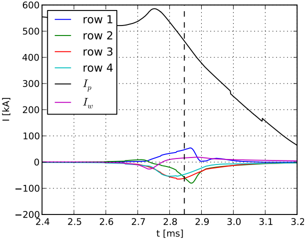

Another M3D-C1 2D nonlinear run of NSTX #132859

with $\eta_W = 5 \times 10^{-4}\Omega m$, $T_h = 24$eV

toroidal current density

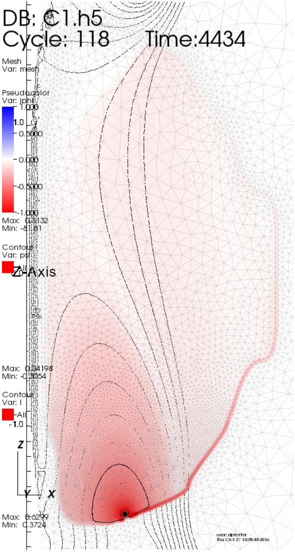

$\vec{B}_{poloidal}$ and j_{normal}

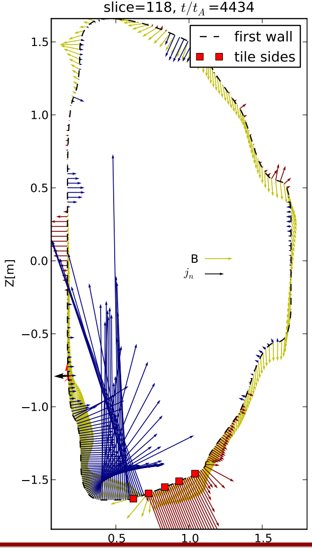

q-profile

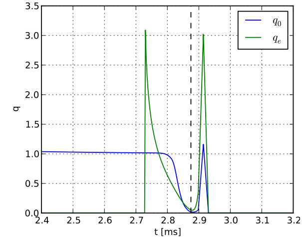

shunt tile currents

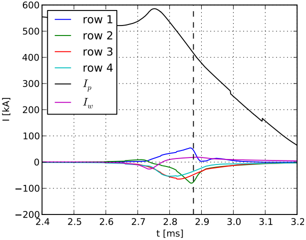

Another M3D-C1 2D nonlinear run of NSTX #13285[9]

with $\eta_W = 5 \times 10^{-4}\Omega m$, $T_h = 24\text{eV}$

toroidal current density

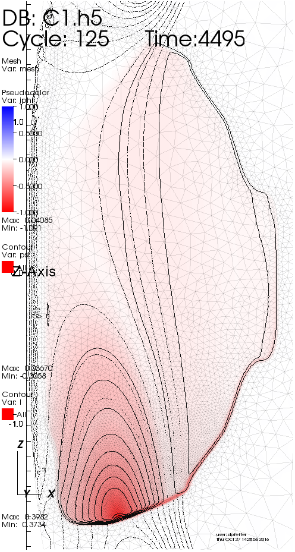

$\vec{B}_{poloidal}$ and j_{normal}

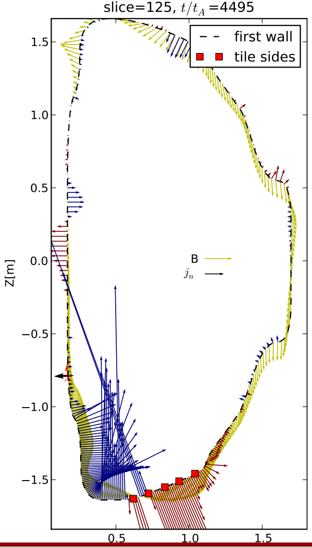

q-profile

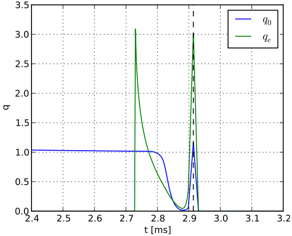

shunt tile currents

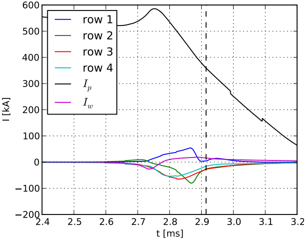

Another M3D-C1 2D nonlinear run of NSTX #132859

with $\eta_W = 5 \times 10^{-4}\Omega m$, $T_h = 24$eV

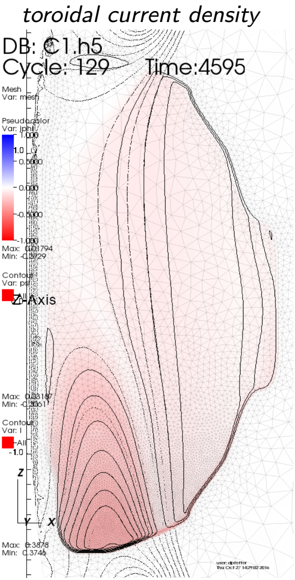

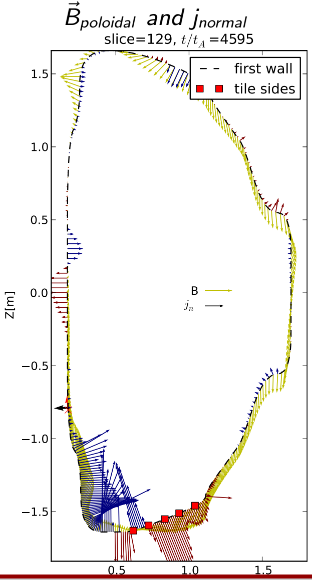

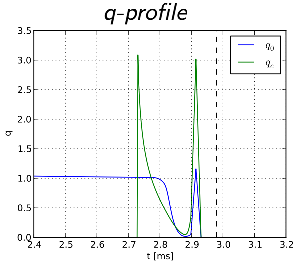

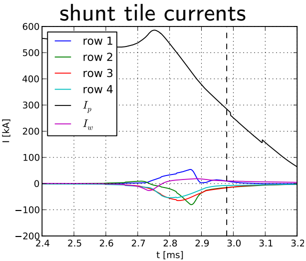

Another M3D-C1 2D nonlinear run of NSTX #132859

with $\eta_W = 5 \times 10^{-4}\Omega m$, $T_h = 24$eV

toroidal current density

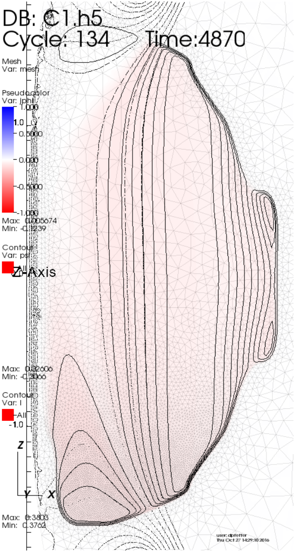

$\vec{B}_{poloidal}$ *and* j_{normal}

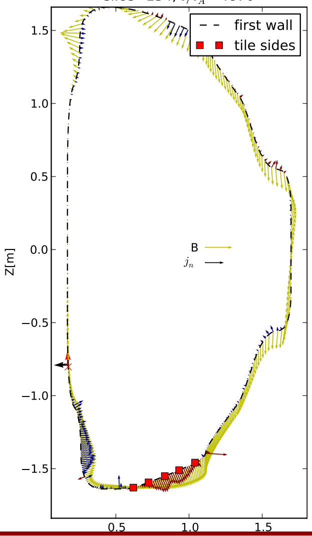

q-profile

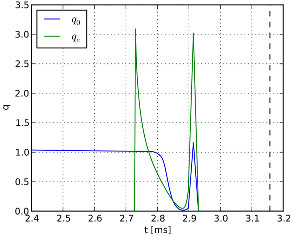

shunt tile currents

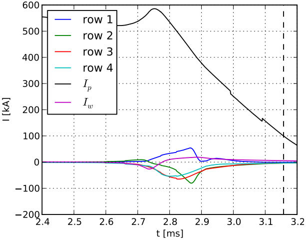

Comments about 2D nonlinear runs

- plasma current is slowly decaying (L_p/R_p) without loop voltage
- current density naturally peaks during slow drift phase $\Rightarrow q_0 < 1$
  - core stability, internal/external inductance (coupling with wall)
  - internal kink can precipitate thermal quench
- $T_h = 9$eV for halo resistivity **reduces induced halo currents**
  - no negative toroidal currents at separatrix
  - plasma current evolution $I_p(t)$ is rounder during quench
    - contact point is narrower $\Rightarrow$ slower flux release
    - later appearance and shorter duration of normal wall currents
  - growth rates decrease with halo temperature (in particular $n = 0$)

Linear analysis informs on non-axisymmetric modes and when to initiate 3D run

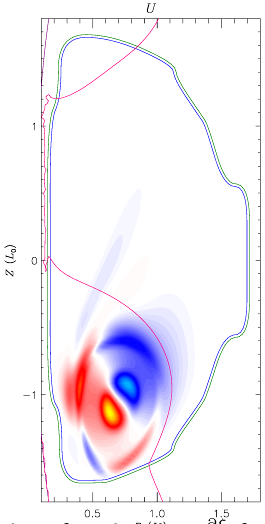

eigen-function $\Phi = \frac{\partial \xi}{\partial t}$ for $n = 1$ at $t = 45300\tau_A$

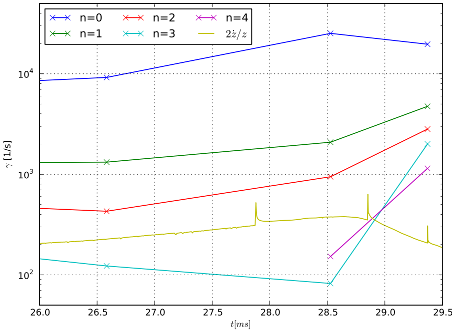

- core modes during drift phase
  - current density peaks causing drop of $q_0 < 1$
  - sawtooth instability could be used as a proxy for thermal quench
- $n = 0$ linear growth-rate from kinetic energy is higher than non-linear evolution of z_{axis}
  - poloidal rotation (sliding) + contraction

3D nonlinear runs launched as plasma contacts wall

Here showing case with $\eta_W = 5 \times 10^{-4}\Omega m$, $T_h = 24$eV

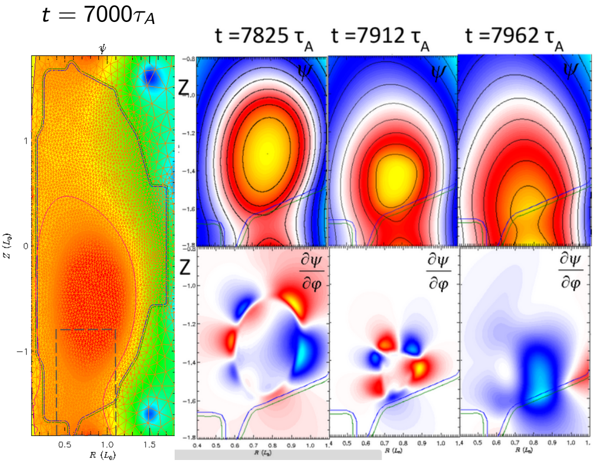

- computationally expensive and sensitive to run
  - 300'000 CPU hours
  - alleviate numerical build-up of gradients via
    - time-step, viscosity, conductivity, resistivity
  - **anisotropic** mesh helps
- non-axisymmetric modes confined to edge
  - halo high temperature, i.e. low resistivity
  - stabilising surface currents
  - stable core to $n > 0$
  - q_e drops below $q_0 \sim 1$

3D nonlinear runs reveal stiff dynamics

Here showing case with $\eta_W = 5 \times 10^{-4}\Omega m$, $T_h = 24$eV

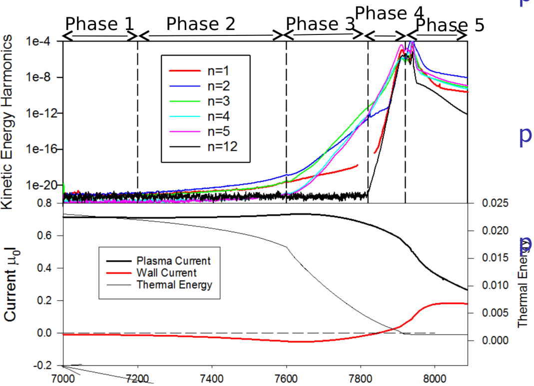

- p.1 drifting plasma (in 3D)
- p.2 vertical motion stalls due to induced $n = 0$ wall currents
  - scrapping-off of LCFS but $q_e > 2$ stable
- p.3 edge surface currents develop as $q_e < 2$
  - stabilise external kink
- p.4 rapid growth of all modes
  - violent termination of plasma as $q_e < 1$
  - complete loss of temperature (flux-surfaces)
- p.5 current decay in residual cold plasma

Virtual diagnostic of 3D normal wall current to compare with shunt tile measurements

normal currents on wall (total)

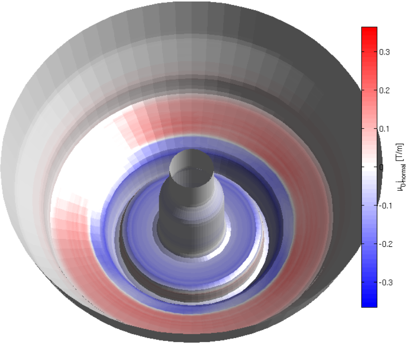

normal currents on wall (non-axisymmetric)

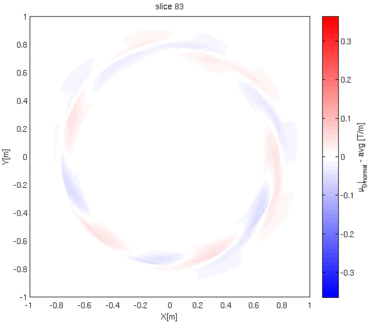

- amplitude quantitatively matches experimental shunt tile
- pattern rotation / zonal component
  - $n = 3 \rightarrow n = 1$, stretching $\rightarrow$ shrinking of current tubes
  - globally zero momentum

1

[1] `C1WC`: post-processing MPI parallelised `FORTRAN` code coupled to `FIO`

Virtual diagnostic of 3D normal wall current to compare with shunt tile measurements

normal currents on wall (total)

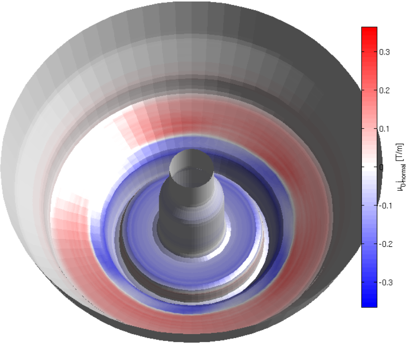

normal currents on wall (non-axisymmetric)

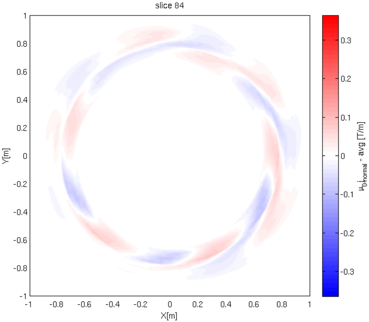

- amplitude quantitatively matches experimental shunt tile
- pattern rotation / zonal component
  - $n = 3 \rightarrow n = 1$, stretching $\rightarrow$ shrinking of current tubes
  - globally zero momentum

1

[1] `C1WC`: post-processing MPI parallelised `FORTRAN` code coupled to `FIO`

Virtual diagnostic of 3D normal wall current to compare with shunt tile measurements

normal currents on wall (total)

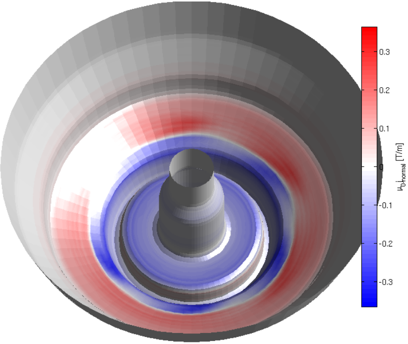

normal currents on wall (non-axisymmetric)

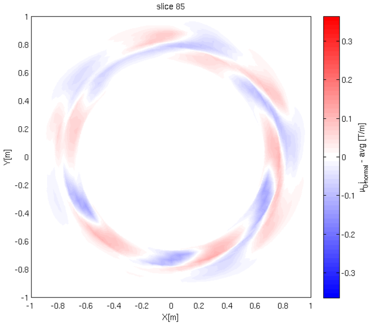

- amplitude quantitatively matches experimental shunt tile
- pattern rotation / zonal component
  - $n = 3 \rightarrow n = 1$, stretching $\rightarrow$ shrinking of current tubes
  - globally zero momentum

1

[1] `C1WC`: post-processing MPI parallelised `FORTRAN` code coupled to `FIO`

Virtual diagnostic of 3D normal wall current to compare with shunt tile measurements

normal currents on wall (total)

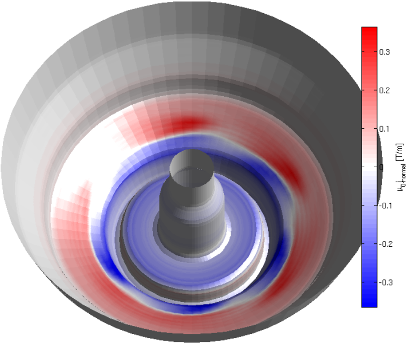

normal currents on wall (non-axisymmetric)

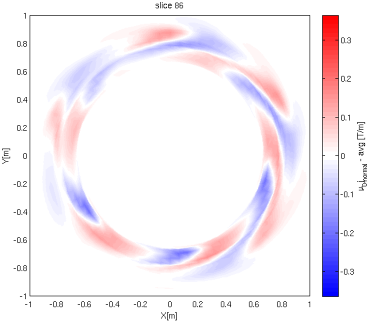

- amplitude quantitatively matches experimental shunt tile
- pattern rotation / zonal component
  - $n = 3 \rightarrow n = 1$, stretching $\rightarrow$ shrinking of current tubes
  - globally zero momentum

1

[1] `C1WC`: post-processing MPI parallelised `FORTRAN` code coupled to `FIO`

Virtual diagnostic of 3D normal wall current to compare with shunt tile measurements

normal currents on wall (total)

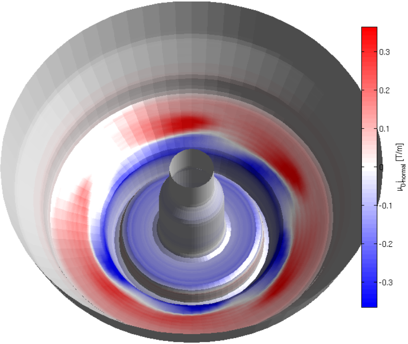

normal currents on wall (non-axisymmetric)

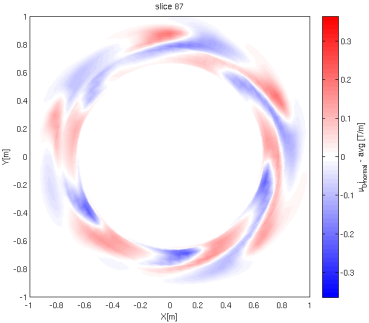

- amplitude quantitatively matches experimental shunt tile
- pattern rotation / zonal component
  - $n = 3 \rightarrow n = 1$, stretching $\rightarrow$ shrinking of current tubes
  - globally zero momentum

1

[1] `C1WC`: post-processing MPI parallelised `FORTRAN` code coupled to `FIO`

Virtual diagnostic of 3D normal wall current to compare with shunt tile measurements

normal currents on wall (total)

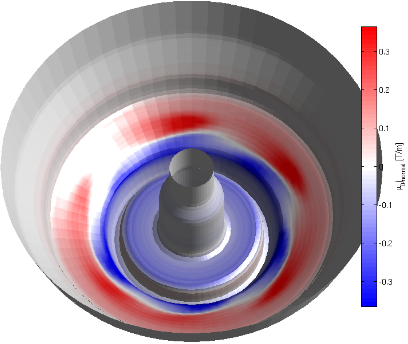

normal currents on wall (non-axisymmetric)

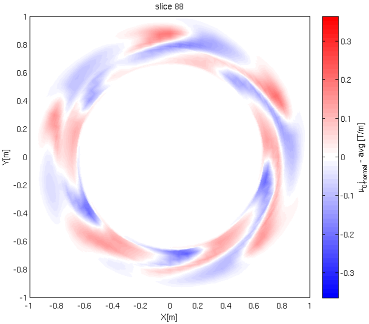

- amplitude quantitatively matches experimental shunt tile
- pattern rotation / zonal component
  - $n = 3 \rightarrow n = 1$, stretching $\rightarrow$ shrinking of current tubes
  - globally zero momentum

1

[1] `C1WC`: post-processing MPI parallelised `FORTRAN` code coupled to `FIO`

Virtual diagnostic of 3D normal wall current to compare with shunt tile measurements

normal currents on wall (total)

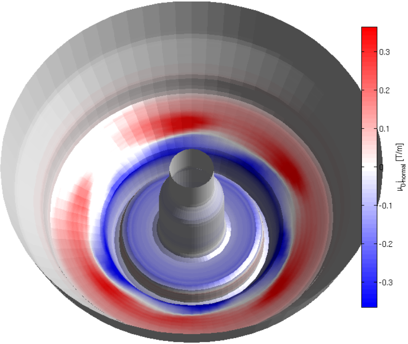

normal currents on wall (non-axisymmetric)

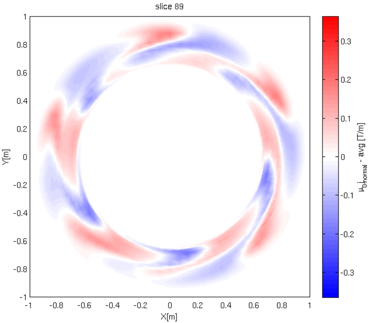

- amplitude quantitatively matches experimental shunt tile
- pattern rotation / zonal component
  - $n = 3 \rightarrow n = 1$, stretching $\rightarrow$ shrinking of current tubes
  - globally zero momentum

1

[1] `C1WC`: post-processing MPI parallelised `FORTRAN` code coupled to `FIO`

Virtual diagnostic of 3D normal wall current to compare with shunt tile measurements

normal currents on wall (total)

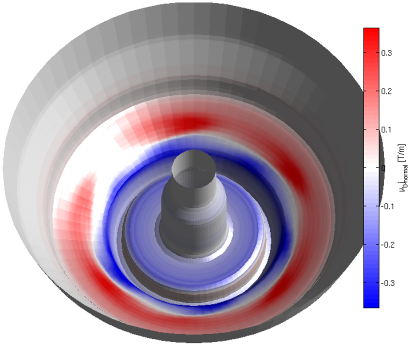

normal currents on wall (non-axisymmetric)

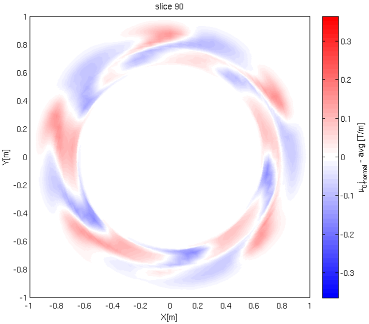

- amplitude quantitatively matches experimental shunt tile
- pattern rotation / zonal component
  - $n = 3 \rightarrow n = 1$, stretching $\rightarrow$ shrinking of current tubes
  - globally zero momentum

1

[1] C1WC: post-processing MPI parallelised FORTRAN code coupled to FIO

Virtual diagnostic of 3D normal wall current to compare with shunt tile measurements

normal currents on wall (total)

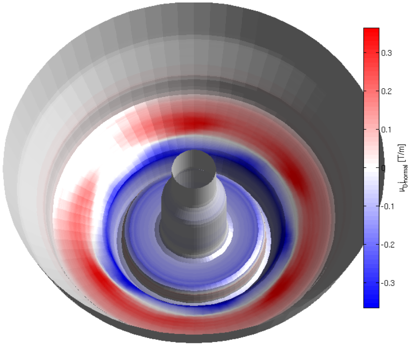

normal currents on wall (non-axisymmetric)

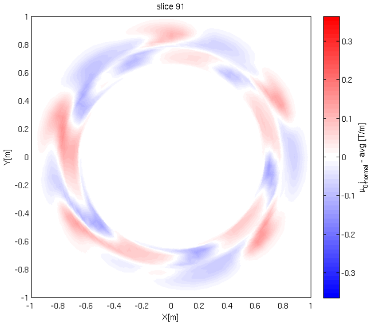

- amplitude quantitatively matches experimental shunt tile
- pattern rotation / zonal component
  - $n = 3 \rightarrow n = 1$, stretching $\rightarrow$ shrinking of current tubes
  - globally zero momentum

1

[1] C1WC: post-processing MPI parallelised FORTRAN code coupled to FIO

Virtual diagnostic of 3D normal wall current to compare with shunt tile measurements

normal currents on wall (total)

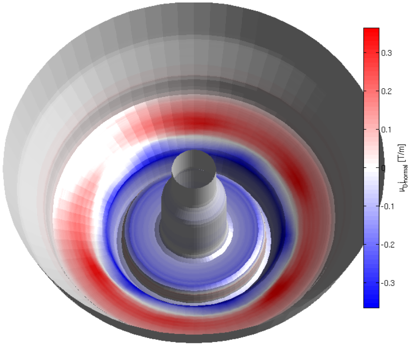

normal currents on wall (non-axisymmetric)

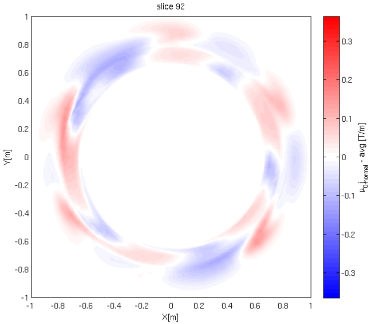

- amplitude quantitatively matches experimental shunt tile
- pattern rotation / zonal component
  - $n = 3 \rightarrow n = 1$, stretching $\rightarrow$ shrinking of current tubes
  - globally zero momentum

1

[1] `C1WC`: post-processing MPI parallelised `FORTRAN` code coupled to `FIO`

Virtual diagnostic of 3D normal wall current to compare with shunt tile measurements

normal currents on wall (total)

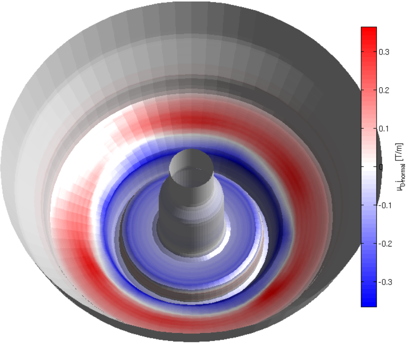

normal currents on wall (non-axisymmetric)

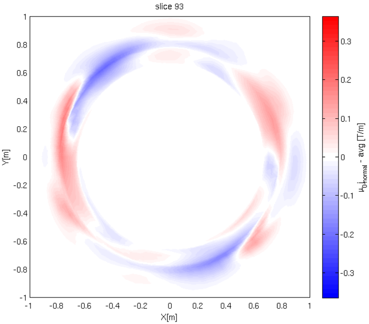

- amplitude quantitatively matches experimental shunt tile
- pattern rotation / zonal component
  - $n = 3 \rightarrow n = 1$, stretching $\rightarrow$ shrinking of current tubes
  - globally zero momentum

1

[1] C1WC: post-processing MPI parallelised FORTRAN code coupled to FIO

Virtual diagnostic of 3D normal wall current to compare with shunt tile measurements

normal currents on wall (total)

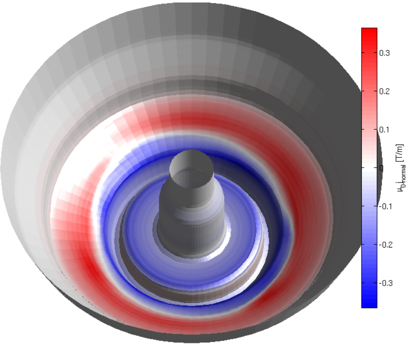

normal currents on wall (non-axisymmetric)

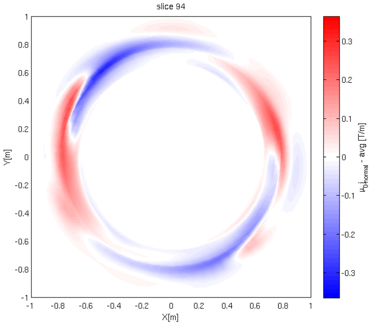

- amplitude quantitatively matches experimental shunt tile
- pattern rotation / zonal component
  - $n = 3 \rightarrow n = 1$, stretching $\rightarrow$ shrinking of current tubes
  - globally zero momentum

1

[1] `C1WC`: post-processing MPI parallelised `FORTRAN` code coupled to `FIO`

Virtual diagnostic of 3D normal wall current to compare with shunt tile measurements

normal currents on wall (total)

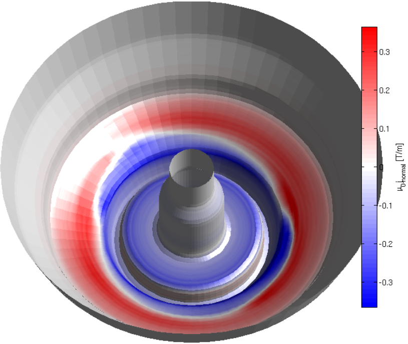

normal currents on wall (non-axisymmetric)

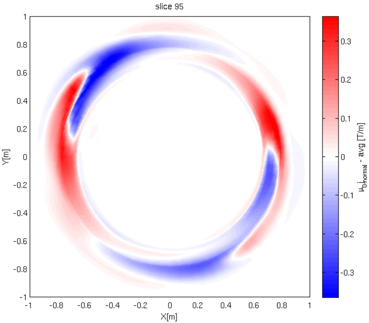

- amplitude quantitatively matches experimental shunt tile
- pattern rotation / zonal component
  - $n = 3 \rightarrow n = 1$, stretching $\rightarrow$ shrinking of current tubes
  - globally zero momentum

1

[1] C1WC: post-processing MPI parallelised FORTRAN code coupled to FIO

Virtual diagnostic of 3D normal wall current to compare with shunt tile measurements

normal currents on wall (total)

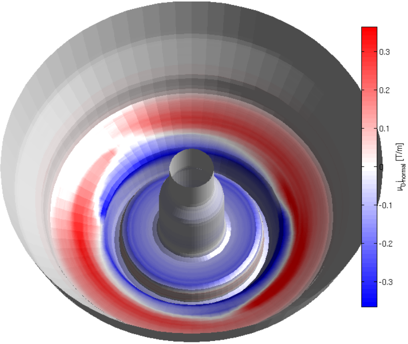

normal currents on wall (non-axisymmetric)

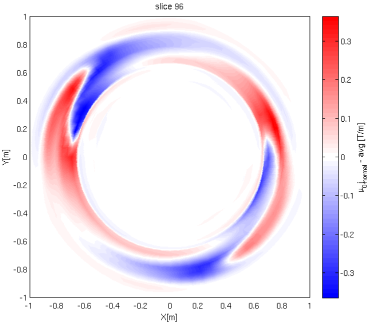

- amplitude quantitatively matches experimental shunt tile
- pattern rotation / zonal component
  - $n = 3 \rightarrow n = 1$, stretching $\rightarrow$ shrinking of current tubes
  - globally zero momentum

1

[1]`C1WC`: post-processing MPI parallelised `FORTRAN` code coupled to `FIO`

Virtual diagnostic of 3D normal wall current to compare with shunt tile measurements

normal currents on wall (total)

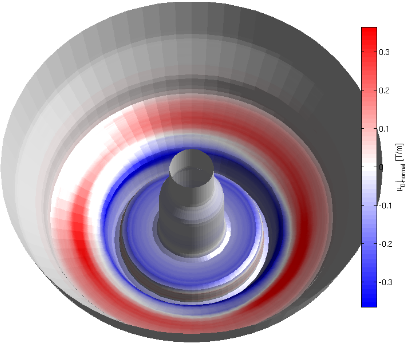

normal currents on wall (non-axisymmetric)

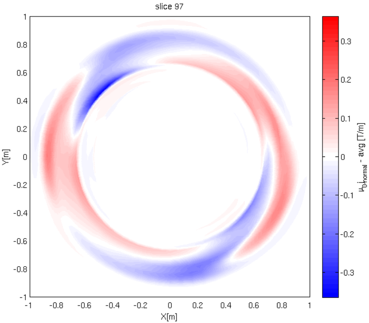

- amplitude quantitatively matches experimental shunt tile
- pattern rotation / zonal component
  - $n = 3 \rightarrow n = 1$, stretching $\rightarrow$ shrinking of current tubes
  - globally zero momentum

1

[1] `C1WC`: post-processing MPI parallelised `FORTRAN` code coupled to `FIO`

Virtual diagnostic of 3D normal wall current to compare with shunt tile measurements

normal currents on wall (total)

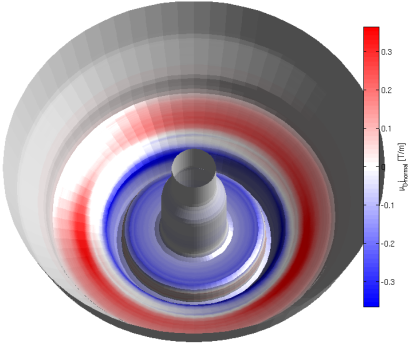

normal currents on wall (non-axisymmetric)

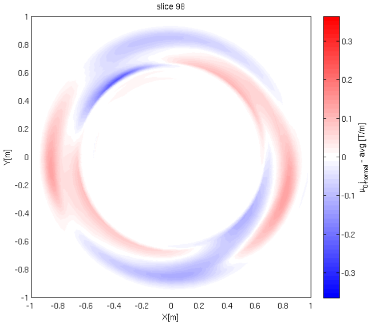

- amplitude quantitatively matches experimental shunt tile
- pattern rotation / zonal component
  - $n = 3 \rightarrow n = 1$, stretching $\rightarrow$ shrinking of current tubes
  - globally zero momentum

1

[1] `C1WC`: post-processing MPI parallelised `FORTRAN` code coupled to `FIO`

Virtual diagnostic of 3D normal wall current to compare with shunt tile measurements

normal currents on wall (total)

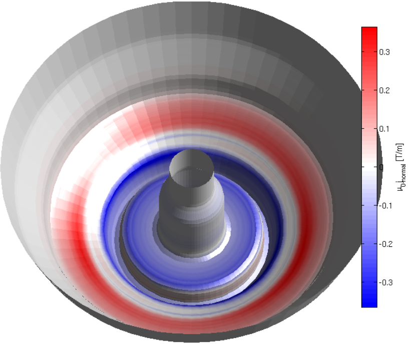

normal currents on wall (non-axisymmetric)

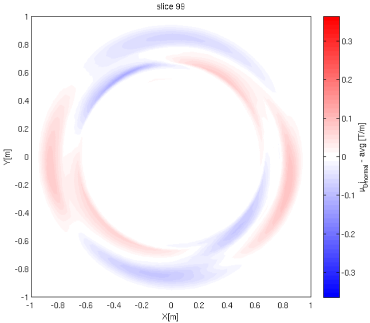

- amplitude quantitatively matches experimental shunt tile
- pattern rotation / zonal component
  - $n = 3 \rightarrow n = 1$, stretching $\rightarrow$ shrinking of current tubes
  - globally zero momentum

1

[1] C1WC: post-processing MPI parallelised FORTRAN code coupled to FIO

Virtual diagnostic of 3D normal wall current to compare with shunt tile measurements

normal currents on wall (total)

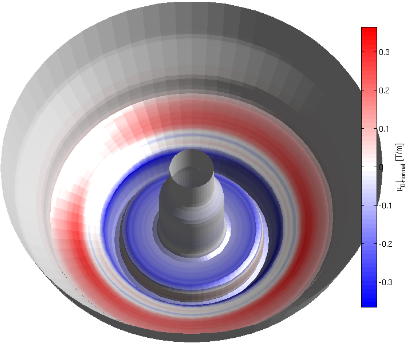

normal currents on wall (non-axisymmetric)

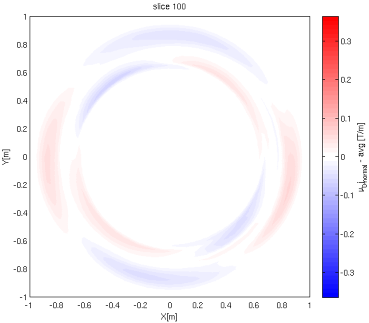

- amplitude quantitatively matches experimental shunt tile
- pattern rotation / zonal component
  - $n = 3 \rightarrow n = 1$, stretching $\rightarrow$ shrinking of current tubes
  - globally zero momentum

1

[1] C1WC: post-processing MPI parallelised FORTRAN code coupled to FIO

Summary and conclusions

- M3D-C1 is employed to model NSTX VDEs with realistic parameters
  - resistive wall capability with finite thickness
  - anisotropic mesh to resolve sharp gradients at plasma/wall contact point
  - implicit scheme to resolve advection-diffusion stiff problem
- faster 2D nonlinear runs are used to meet experimental timescales
- linear analysis to assess growth and structure of non-axisymmetric modes
- massive 3D nonlinear runs for evolution/saturation of non-axisymmetric wall currents
- virtual diagnostics of normal wall currents to compare with experimental data

Ongoing work and future plans

- Simulations, numerics
  - more 2D runs: fine-tuning of wall resistivity, halo temperature, heat conductivity, loop voltage,...
  - as many 3D runs as possible: convergence with toroidal planes, timing of 2D to 3D switching, smoothing/damping of numerical instabilities,...
- Analysis, interpretation and comparison with experimental data
  - sequence of events (z_{mag}, total currents, q-profile) + linear study
  - halo currents, wall forces, mode rotation, torque, TPF,...
  - virtual diagnostics for shunt tiles + magnetic probes
- Extensions and additional effects
  - CHI gap (enforce zero poloidal wall currents)
  - non-uniform / non-axisymmetric wall resistivity
  - toroidal rotation, torque, plasma/wall boundary conditions, sheath physics

Bibliography I

D. Pfefferlé, PPPL (2016).

X. Wesley, Journal (2006).

C. Myers, PPPL (2016).